

One-Shot Federated Learning with Classifier-Guided Diffusion Models

Mingzhao Yang ^{*}, Shangchao Su ^{*}, Bin Li [†], Xiangyang Xue

Fudan University, Shanghai, China
 {mzyang20,scsu20,libin,xyxue}@fudan.edu.cn

Abstract

One-shot federated learning (OSFL) has gained attention in recent years due to its low communication cost. However, most of the existing methods require auxiliary datasets or training generators, which hinders their practicality in real-world scenarios. In this paper, we explore the novel opportunities that diffusion models bring to OSFL and propose FedCADO, utilizing guidance from client classifiers to generate data that complies with clients' distributions and subsequently training the aggregated model on the server. Specifically, our method involves targeted optimizations in two aspects. On one hand, we conditionally edit the randomly sampled initial noises, embedding them with specified semantics and distributions, resulting in a significant improvement in both the quality and stability of generation. On the other hand, we employ the BN statistics from the classifiers to provide detailed guidance during generation. These tailored optimizations enable us to limitlessly generate datasets, which closely resemble the distribution and quality of the original client dataset. Our method effectively handles the heterogeneous client models and the problems of non-IID features or labels. In terms of privacy protection, our method avoids training any generator or transferring any auxiliary information on clients, eliminating any additional privacy leakage risks. Leveraging the extensive knowledge stored in the pre-trained diffusion model, the synthetic datasets can assist us in surpassing the knowledge limitations of the client samples, resulting in aggregation models that even outperform the performance ceiling of centralized training in some cases, which is convincingly demonstrated in the sufficient quantification and visualization experiments conducted on three large-scale multi-domain image datasets.

1 Introduction

Federated learning (FL) (McMahan et al. 2017) has gained increasing attention recently. Standard FL relies on frequent communication between the server and clients. With the growing adoption of AI models by individual users, the application scenarios of FL have expanded significantly, including mobile photo album categorization and autonomous driving (Nguyen et al. 2022; Fantauzzo et al. 2022). However, in these scenarios, the substantial communication cost associated with FL is often impractical for individual users. As a result, one-shot FL (OSFL) has emerged as a solution. OSFL

aims to establish the aggregated model within a single communication round. Currently, mainstream OSFL methods can be categorized into three types: 1) Methods using the public auxiliary dataset (Guha, Talwalkar, and Smith 2019; Li, He, and Song 2020; Lin et al. 2020). 2) Methods training generators (Zhang et al. 2022a; Heinbaugh, Luz-Ricca, and Shao 2022). 3) Methods transferring auxiliary information (Zhou et al. 2020; Su, Li, and Xue 2023).

However, existing methods are hard to apply in real-world scenarios due to the following reasons: **1)** Collecting public datasets on the server that comply with all client distribution is impractical, owing to privacy concerns and data diversity issues. **2)** Generating data that comply with client distributions is challenging. In real scenarios, client devices often have limited data. Moreover, training generators for realistic images is inherently difficult. So most OSFL methods can only be applied to small-scale toy datasets, such as MNIST and CIFAR10. **3)** Existing one-shot methods focus on label distribution skew (i.e., differences in $p(y)$) while neglecting feature distribution skew (i.e., $p(\mathbf{x}|y)$). This further restricts their applicability. In light of these challenges, this paper aims to reconsider the establishment of a **practical one-shot FL framework specifically tailored to real-world scenarios**.

With the remarkable performance of diffusion models (DM) in AIGC, a lot of pre-trained DMs containing vast knowledge have emerged. Applying these pre-trained DMs in FL holds immense potential for addressing the issues encountered by existing OSFL methods: Firstly, with proper guidance, DMs can generate images that resemble the client's personalized distribution without accessing private client data, eliminating the need for any public dataset or additional information transfer. Secondly, due to the high-quality generation capabilities of DMs, we can transition from toy datasets to realistic datasets, enhancing the practical value of OSFL. Thirdly, pre-trained DMs can generate images with sufficient variety in both categories and distributions, enabling the capability to address the complex situations that arise in various real-world scenarios such as feature skew and heterogeneous client models.

Moreover, applying pre-trained DMs within FL offers a significant advantage – the potential to break through the performance ceiling of traditional FL. In FL, an inaccessible ceiling involves uploading all client images to the server for centralized training, yet even this ceiling is limited by

^{*}These authors contributed equally.

[†]Corresponding author

the knowledge within the client samples. However, with the assistance of pre-trained DMs with vast knowledge, the FL methods hold the potential to surpass this ceiling. Therefore, the integration of pre-trained DMs and FL could potentially become a crucial avenue for the future of FL. On this avenue, a pivotal step is guiding the pre-trained DMs to generate data that complies with the personalized client distributions.

Given the above motivations, we propose **FedCADO**, a **Classifier-Assisted Diffusion for One-shot Federated** learning method. The core idea of FedCADO involves using the classifiers $\{\mathcal{F}_{\theta_k}\}_{k=1}^K$, which are trained and uploaded by the clients, as conditions to guide the pre-trained DM in generation. However, conventional classifier guidance (Dhariwal and Nichol 2021) only focuses on semantics, making it fall short in OSFL scenarios. Therefore, we primarily implemented two optimizations for it.

Firstly, we introduce a step of **initial noise editing** before denoising. This step involves embedding semantic and distributional information into the initial noise, effectively reducing the complexity of generation and significantly enhancing its quality and stability. Secondly, we employ both the **classifiers** and the **statistics** of their batch normalization (BN) layers to provide detailed guidance about client distributions. The addition of these statistics minimizes the distance between the client distribution and the synthetic distribution, further guaranteeing the semantic and distributional information of generated samples. These tailored optimizations enable us to limitlessly generate datasets, which closely resemble the distribution and quality of the client dataset.

After obtaining the synthetic dataset, we present three approaches to obtain the aggregated model: fine-tuning, multi-teacher distillation, and specific-teacher distillation. Through these approaches, we achieve the model aggregation with one round of communication. Importantly, our method works without accessing any client data and avoids any additional information transfer compared with standard FL, ensuring the prevention of additional privacy leaks.

To validate the performance of our method, we conduct extensive quantitation and visualization experiments on three large-scale real image datasets: DomainNet (Peng et al. 2019), OpenImage (Kuznetsova et al. 2020) and NICO++ (Zhang et al. 2022b), providing strong evidence for our aforementioned ideas. Sufficient visualization experiments demonstrate that our method generates synthetic datasets that comply with both the specific categories and the personalized client distributions, with comparable quality and diversity to the original client dataset, and even surpassing it in certain domains. Quantitation experiments under various client scenarios further demonstrate that our method outperforms all baselines in a single communication round, and in some cases even surpasses the ceiling performance. These results strongly underscore the potential application of the DM in the context of federated learning.

In summary, this paper makes the following contributions:

- We propose FedCADO that introduces classifier-guided DMs into OSFL. Our method successfully extends the existing OSFL paradigm from simple toy dataset scenarios to real-world, large-scale complex scenarios, greatly broadening the practicality of OSFL.

- We optimize the classifier-guided diffusion generation by employing the BN statistics of classifiers as guidance and editing the randomly sampled initial noise before the iterative denoising, which effectively enhances the quality and stability of generation and allows us to generate images that not only comply with client personalized distributions but also possess accurate semantic information.
- We conduct extensive experiments on large-scale real-world datasets, including DomainNet, OpenImage, and NICO++. The results demonstrate that our method can train an aggregated model within a single communication round that outperforms other baseline methods, and in some domains, even surpasses the performance ceiling.

2 Related Work

2.1 One-shot Federated Learning

In the standard federated learning (McMahan et al. 2017) setup, there are multiple rounds of communication between the server and clients. To reduce the high communication costs, one-shot federated learning (OSFL) entails clients training their local models to convergence first, followed by aggregation on the server. Existing OSFL methods can be broadly categorized into three main types. **1) Methods based on public auxiliary dataset.** (Guha, Talwalkar, and Smith 2019) utilizes unlabeled public data on the server for model distillation. Similarly, FedKT (Li, He, and Song 2020) and FedDF (Lin et al. 2020) employ an auxiliary dataset for knowledge transfer on the server. **2) Methods based on generators.** DENSE (Zhang et al. 2022a) employs an ensemble of client models as a discriminator to train a generator for generating pseudo samples, which is used to train the aggregated model. To address very high statistical heterogeneity, FedCVAE (Heinbaugh, Luz-Ricca, and Shao 2022) trains a conditional variational autoencoder (CVAE) on the client side and sends the decoders to the server to generate data. **3) Methods based on sharing auxiliary information.** DOSFL (Zhou et al. 2020) performs data distillation on the client, and the distilled pseudo samples are uploaded to the server for global model training. MAEcho (Su, Li, and Xue 2023) shares the orthogonal projection matrices of client features to the server to optimize global model parameters.

2.2 Diffusion Model

The diffusion model (DM) is initially introduced in the work by (Sohl-Dickstein et al. 2015). (Ho, Jain, and Abbeel 2020) proposes the fundamental framework of the DM that we currently employ. Following this, a series of sampling techniques emerge (Song, Meng, and Ermon 2020; Liu et al. 2022; Song et al. 2020; Gu et al. 2022), leading to the success of DMs in generation (Kingma et al. 2021; Dhariwal and Nichol 2021; Wang et al. 2018). Subsequently, Stable Diffusion (Rombach et al. 2022) provides a series of high-performance pre-trained DM capable of generating images complying with the majority of common real-world distributions.

One prominent advantage of DMs is their conditional generation capability. Such conditional DMs can be broadly categorized into two types. The first type mainly provides image (Saharia et al. 2022a; Wang et al. 2022; Su et al. 2022;

Zhang and Agrawala 2023) or text (Nichol et al. 2021; Saharia et al. 2022b; Kim, Kwon, and Ye 2022; Preechakul et al. 2022) guidance during the training of the DMs, requiring additional training costs. The second type involves the guidance during generation (Feng et al. 2022; Xie et al. 2023). A prominent example is classifier-guidance (Dhariwal and Nichol 2021). In addition, recent research (Mao, Wang, and Aizawa 2023) also proposes the use of editing the initial noise. These methods do not necessitate additional training and seamlessly integrate DMs with FL because the majority of FL frameworks permit the upload of local client classifiers, which inspires the central idea of our method.

2.3 FL with Pre-trained Diffusion Models

Currently, only a small number of studies have focused on the significant potential of pre-trained DMs in FL. In FedDisc (Yang et al. 2023), stable diffusion is introduced into semi-supervised FL for the first time, achieving remarkable results within just a single communication round. However, it requires using the CLIP image branch as the backbone for classification, which limits its flexibility. FGL (Zhang, Qi, and Zhao 2023) employ BLIPv2 (Li et al. 2023) on the client side to extract image descriptions, from which prompts are extracted and sent to the server for generation using DMs. This approach necessitates pre-deploying BLIPv2 on the client side. Phoenix (Jothiraj and Mashhadi 2023) introduced FL into DMs, proposing a distributed method for training DMs. Unlike FedDisc and FGL, we do not require deploying any foundational models on the clients, which further enhances the practicality of our method and enables our method to address the scenario of heterogeneous client models.

3 Method

The overall process of FedCADO is depicted in Figure 1. In Section 3.1, we provide some essential preliminaries about FedCADO. In Section 3.2, we elaborate on the conditional sampling of our method, involving how we guide image generation by both class label and batch normalization. In Section 3.3, we outline the process of image generation in two steps: initial noise editing and diffusion denoising. In Section 3.4, we enumerate three strategies employed to accomplish model aggregation based on the generated images.

3.1 Preliminaries

Diffusion Process The DM ϵ_θ samples initial noise \mathbf{s}_T from a standard Gaussian distribution $\mathcal{N}(0, \mathcal{I})$ and iteratively denoises it, resulting in a realistic image \mathbf{s}_0 , where T denotes the max time step in iteration. (Dhariwal and Nichol 2021) proposes the classifier-guidance of diffusion, wherein the gradients backpropagated through the classifier \mathcal{F}_{θ_k} are used to modify the predicted noise of the DM $\epsilon_\theta(\mathbf{s}_t, t)$ at each time step. The loss function utilized for generating gradients typically involves the cross-entropy loss \mathcal{L}_{CE} between the given class label y and the prediction of classifier $\mathcal{F}_{\theta_k}(\mathbf{s}_t)$. This enables the DM to generate images with specified class label y . With its textual prompt introduced as additional conditions, the sampling process at each time step can be divided into two steps. Firstly, for any given time step $t \in \{0, \dots, T\}$,

the predicted noise is modified according to the following equation:

$$\hat{\epsilon}(\mathbf{s}_t, t|y) := \epsilon_\theta(\mathbf{s}_t, t|y) - \sqrt{1 - \alpha_t} \nabla_{\mathbf{s}_t} \log p_{\theta_k}(y|\mathbf{s}_t) \quad (1)$$

Afterwards, utilizing the modified $\hat{\epsilon}(\mathbf{s}_t, t|y)$, the sample for the next time step \mathbf{s}_{t-1} is obtained:

$$\begin{aligned} \mathbf{s}_{t-1} = & \sqrt{\alpha_{t-1}} \left(\frac{\mathbf{s}_t - \sqrt{1 - \alpha_t} \hat{\epsilon}(\mathbf{s}_t, t|y)}{\sqrt{\alpha_t}} \right) \\ & + \sqrt{1 - \alpha_{t-1} - \sigma_t^2} \cdot \hat{\epsilon}(\mathbf{s}_t, t|y) + \sigma_t \varepsilon_t \end{aligned} \quad (2)$$

where α_t , α_{t-1} and σ_t are pre-defined parameters, ε_t is the Gaussian noise randomly sampled at each timestep.

Problem Setting and Notation Consider that we have K clients. In OSFL, take client k as an example, this client has a private dataset $\mathcal{D}^k = \{(\mathbf{x}_i, y_i)\}_{i=1}^{N_k}$, trains the classifier \mathcal{F}_{θ_k} to convergence on \mathcal{D}^k and sends it to the server. The server needs to aggregate the models $\{\mathcal{F}_{\theta_k}\}_{k=1}^K$ to obtain an aggregated model \mathcal{F}_{θ_g} that adapts various client distributions.

3.2 Conditional Sampling

In this section, we elaborate on how the classifiers uploaded by the clients guide us in conducting conditional sampling. Diverging from the conventional classifier-guidance, in our problem setting, generated images must possess accurate categories and comply with specified client distributions. This introduces novel demands to conditional sampling, necessitating consideration of additional image attributes such as style, color, background, etc. Relying solely on classifiers falls significantly short of achieving these criteria.

To provide detailed information to the server’s generation, we deliberate on the statistics of each batch normalization (BN) layer of classifier \mathcal{F}_{θ_k} : mean and variance. In other words, we need to consider the conditional sampling process $p(\mathbf{s}_{t-1}|\mathbf{s}_t, y, \{\mu_{k,l}\}_{l=1}^{L_k}, \{\sigma_{k,l}^2\}_{l=1}^{L_k})$, where $\mu_{k,l}$ and $\sigma_{k,l}^2$ respectively denote the means and the variances of all BN layers within \mathcal{F}_{θ_k} , and L_k represents the number of BN layers within \mathcal{F}_{θ_k} . Therefore, during modifying the predicted noise of the DM $\epsilon_\theta(\mathbf{s}_t, t|y)$ at each time step t , we compute gradients by summing the cross-entropy loss \mathcal{L}_{CE} and the BN Loss \mathcal{L}_{BN} to incorporate the additional distribution details embedded within the statistics of the BN layers into the diffusion process. The computation of \mathcal{L}_{BN} is as follows:

$$\mathcal{L}_{BN}(\mathbf{s}, \theta_k) = \sum_{l=1}^L (\|\mu_l(\mathbf{s}, \theta_k) - \mu_{k,l}\| + \|\sigma_l^2(\mathbf{s}, \theta_k) - \sigma_{k,l}^2\|)$$

where $\mu_l(\mathbf{s}, \theta_k)$ and $\sigma_l^2(\mathbf{s}, \theta_k)$ denote the mean and variance of the output feature from the l th BN layer after feeding the sample \mathbf{s} into the classifier \mathcal{F}_{θ_k} .

Furthermore, since classifiers are simply trained on the client \mathcal{F}_{θ_k} and are not accustomed to the direct input of \mathbf{s}_t , which has high levels of noise, traditional classifier-guidance struggles to provide accurate guidance to the generation process through the computed gradient $\nabla_{\mathbf{s}_t} \log p_{\theta_k}(y|\mathbf{s}_t)$. To address this challenge, inspired by (Song, Meng, and Ermon 2020), at any time step t , we utilize the predicted noise of

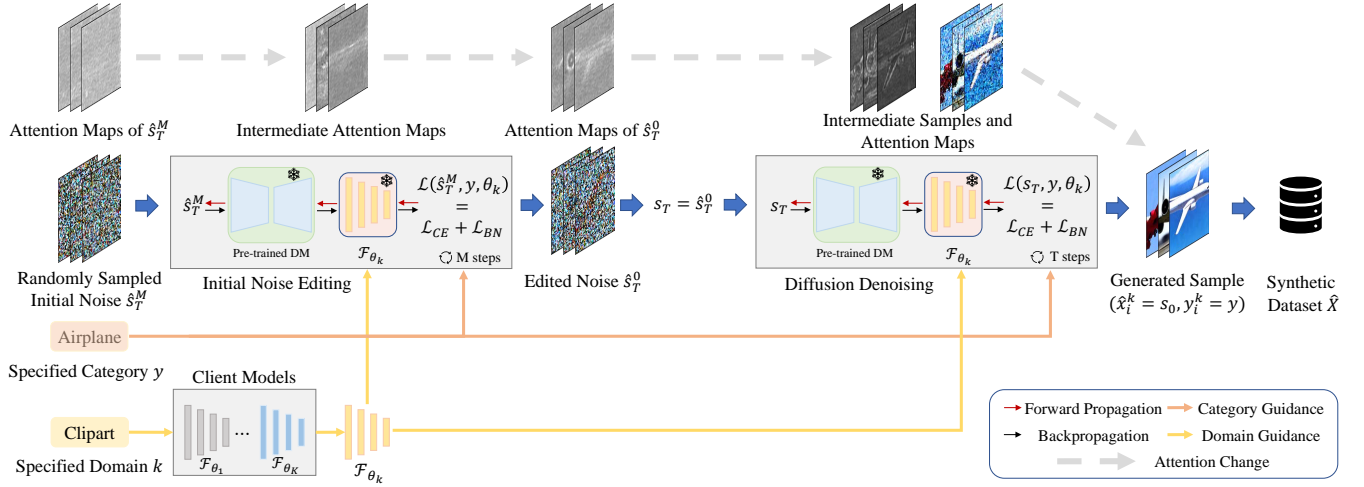


Figure 1: Overview of our FedCADO. With the specified domain, we first select the classifier from the clients’ models. Guided by the provided labels, classifier, and BN statistics, we edit the randomly sampled initial noise to embed the given semantic and distributional information in it. Subsequently, we iteratively denoise the edited noise, resulting in the generation of images. The changes in attention reveal that the initial noise editing predefines the rough outline of objects, effectively enhancing the quality and stability of the denoising process.

the DM $\epsilon_\theta(s_t, t|y)$ to predict s_0 according to the following equation:

$$\hat{s}_{0,t} = \frac{s_t - \sqrt{1 - \alpha_t} \hat{\epsilon}(s_t, t|y)}{\sqrt{\alpha_t}} \quad (3)$$

Subsequently, based on $\hat{s}_{0,t}$, we compute the loss function and gradient to modify $\epsilon_\theta(s_t, t|y)$. Although in the initial time steps, $\hat{s}_{0,t}$ may appear blurry, the noise level in comparison to s_t is noticeably reduced. This decreases the demand for the classifier’s robustness about noise, mitigating the need for clients to specifically train for classifying noised samples.

In summary, the overall loss function \mathcal{L} employed in the conditional sampling is as follows:

$$\mathcal{L}(s_t, y, \theta_k) = \mathcal{L}_{CE}(\mathcal{F}_{\theta_k}(\hat{s}_{0,t}), y) + \lambda \mathcal{L}_{BN}(\hat{s}_{0,t}, \theta_k) \quad (4)$$

After performing gradient backpropagation according to this loss function, we use Equations (1) and (2) to guide the generation process through the classifier \mathcal{F}_{θ_k} and its accompanying BN layer statistics, enabling conditional sampling.

3.3 Image Generation

Compared with the traditional classifier-guidance, we also optimize the image generation for the problem setting of OSFL, involving partitioning the generation process into two stages: initial noise editing and diffusion denoising.

Initial Noise Editing After the random sampling of initial noise s_T , we find that directly proceeding with denoising led to unstable results. In our analysis, the variation in the quality of generated results can be attributed to the stochasticity of the initial noise. Throughout the diffusion process, a substantial correlation exists between the generated samples and the initial noise, leading to instances where some initial noises

are challenging to denoise into realistic images that comply with specified categories and distribution. Consequently, with the inspiration of (Mao, Wang, and Aizawa 2023), we incorporate a step of initial noise editing before the diffusion denoising process. To enhance the quality and stability of the entire generation process, editing the initial noise involves injecting specific semantic information into the initial noise, which guides the subsequent denoising process to generate images that comply with our desired distribution more easily.

In a more detailed exposition, analogous to the classifier-guidance expounded in Section 3.1, at time step T , given the randomly sampled initial noise s_T , category label y , and domain label k , we compute the gradients based on the loss function in Equation 3. However, following this computation, we do not modify the predicted noise of DM $\epsilon_\theta(s_T, T|y)$ and iterate to the next time step $T - 1$. Instead, we iteratively edit s_T with the computed gradient for M steps:

$$\hat{s}_T^{m-1} = \hat{s}_T^m - \eta \nabla_{\hat{s}_T^m} \mathcal{L}(\hat{s}_T^{m-1}, y, \theta_k), m = 1, \dots, M$$

During the process of editing the initial noise, noticeable reductions in \mathcal{L}_{CE} and \mathcal{L}_{BN} are observed, indicating that the initial noise is incorporated with the information about the specified category and distribution, leading to a noticeable reduction in denoising difficulty. Therefore, generating images based on the edited initial noise substantially enhances the stability of generated samples. The practical effect of initial noise editing is presented in the quantitative and visual ablation experiments in Table 3 and Figure 4.

Diffusion Denoising After obtaining the edited initial noise \hat{s}_T^M , we utilize \hat{s}_T^M as the DM’s initial noise s_T and proceed with the diffusion denoising procedure. we proceed to the step of diffusion denoising. Similar to the process described in Section 3.1, for any given time step $t \in \{0, \dots, T\}$, we

		OpenImage							DomainNet						
		client0	client1	client2	client3	client4	client5	Avg	clipart	infograph	painting	real	sketch	Avg	
Baselines	Ceiling	49.88	50.56	57.89	59.96	66.53	51.38	56.03	62.54	29.42	52.96	70.13	53.04	53.62	
	SD_Gen	30.41	30.23	42.92	43.48	50.75	33.43	38.54	28.49	8.36	34.43	70.43	20.50	32.44	
	FedAvg	41.46	50.36	52.61	50.36	62.10	50.17	51.18	48.19	20.01	47.79	67.33	35.97	43.86	
	FedDF	44.96	46.15	59.69	58.69	63.45	46.63	53.26	47.18	16.09	46.13	69.37	30.89	41.93	
Ours	FedCADO_FT	48.99	51.66	55.59	52.80	62.41	58.86	55.05	51.86	22.11	48.63	68.96	41.73	46.66	
	FedCADO_SD	47.60	55.20	61.54	61.83	67.07	59.90	58.86	52.75	23.62	50.24	68.98	43.74	47.87	
	FedCADO_MD	44.70	53.08	58.67	60.13	64.06	58.06	56.45	54.20	23.75	50.36	70.32	42.62	48.25	
		Unique NICO++							Common NICO++						
		client0	client1	client2	client3	client4	client5	Avg	autumn	dim	grass	outdoor	rock	water	Avg
Baselines	Ceiling	79.16	81.51	76.04	72.91	79.16	79.29	78.01	62.66	54.07	64.89	63.04	61.08	54.63	60.06
	SD_Gen	69.79	69.14	69.32	59.89	67.70	66.60	67.07	50.51	38.10	54.53	49.39	49.12	41.58	47.21
	FedAvg	67.31	74.73	69.01	64.37	73.07	67.87	69.39	52.51	40.45	57.21	51.59	49.31	43.56	49.11
	FedDF	69.79	78.90	69.53	66.01	74.86	70.80	71.65	50.44	39.62	57.42	52.91	51.61	44.76	49.46
Ours	FedCADO_FT	75.13	73.30	70.31	68.88	73.60	72.51	72.29	54.63	49.21	58.13	54.75	54.64	47.03	53.07
	FedCADO_SD	77.34	79.94	75.01	71.87	76.69	74.92	75.96	61.49	51.47	65.28	60.03	59.57	51.14	58.16
	FedCADO_MD	74.66	75.78	71.05	69.58	74.34	72.11	72.92	54.42	47.83	59.85	53.94	52.96	45.15	52.36

Table 1: Performance of different methods on OpenImage, DomainNet, Unique NICO++, and Common NICO++ under feature distribution skew, where italicized text represents the ceiling performance used solely as a reference, and bold text signifies the optimal performance excluding the ceiling performance.

modify the predicted noise of the DM based on the loss function mentioned in Equation (4), following the formula provided below.

$$\hat{\epsilon}(\mathbf{s}_t, t|y) := \epsilon_\theta(\mathbf{s}_t, t|y) - \sqrt{1 - \bar{\alpha}_t} \nabla_{\mathbf{s}_t} \mathcal{L}(\mathbf{s}_t, y, \theta_k) \quad (5)$$

Subsequently, based on Equation (2), we compute \mathbf{s}_{t-1} using the modified $\hat{\epsilon}(\mathbf{s}_t, t|y)$, iteratively leading to the realistic image \mathbf{s}_0 . During the generation, since we specify the class y and the classifier \mathcal{F}_{θ_k} , the generated image \mathbf{s}_0 naturally has the class label y and domain label k . We define \mathbf{s}_0 as $\hat{\mathbf{x}}_i^k$ and include along with its class label y_i^k in the synthetic dataset $\hat{\mathbf{X}}$, where i denotes the number of images generated under the guidance \mathcal{F}_{θ_k} . After undergoing multiple iterations of generation, we obtain the synthetic dataset $\hat{\mathbf{X}} = \{(\hat{\mathbf{x}}_i^k, y_i^k)\}_{i=1}^N$.

3.4 Model Aggregation

Based on the synthetic dataset $\hat{\mathbf{X}}$, we proceed to obtain the aggregated model. In this section, we employ the idea of distillation to achieve model aggregation. Given the synthetic sample $\hat{\mathbf{x}}_i^k$ and its class label y_i^k , we delineate three approaches to obtain the aggregated model used in the following experiments: **Fine-tuning**, **Multi-teacher distillation**, and **Specific-teacher distillation**, based on the following aggregation loss function:

$$\mathcal{L}_{agg}(\hat{\mathbf{x}}_i^k, y_i^k) = \mathcal{L}_{CE}(\mathcal{F}_{\theta_g}(\hat{\mathbf{x}}_i^k), y_i^k) + \lambda D_{KL}(\mathcal{F}_{\theta_g}(\hat{\mathbf{x}}_i^k) || \sum_{h=1}^K w_h \mathcal{F}_{\theta_h}(\hat{\mathbf{x}}_i^k)) \quad (6)$$

where D_{KL} means Kullback-Leibler divergence, \mathcal{F}_{θ_g} and $\{\mathcal{F}_{\theta_h}\}_{h=1}^K$ are the aggregated model and client models, $\{w_h\}_{h=1}^K$ are the weights of each client's teacher model, λ is the weight of distillation loss.

Fine-tuning This approach refers to the scenario where λ is set to 0. Since the performance ceiling of centralized training also involves training the aggregated model on the client-uploaded images using cross-entropy loss \mathcal{L}_{CE} , this method can directly reflect the performance difference between the synthetic dataset and the original client dataset.

Multi-teacher Distillation This approach refers to setting the λ to 1 and the weights for all client teacher models to $\frac{1}{K}$, learning knowledge from all teacher models collectively. However, it is not suitable under label distribution skew.

Specific-teacher Distillation Given that $\hat{\mathbf{x}}_i^k$ with both class label y_i^k and domain labels k , we can use the specific teacher model \mathcal{F}_{θ_k} from domain k to guide in its specialized domains and achieve model aggregation, setting the λ to 1 and the weight of \mathcal{F}_{θ_k} is 1, while the rest are all set to 0.

4 Experiments

We aim to answer the following questions in this section: 1) How does the quality of generated data compare to the original client images? 2) Can our method work well on feature skew, label skew, or heterogeneous client models? 3) How does the performance of the aggregated model trained using our method compare to other SOTA methods? 4) What roles do the different factors in our method play? 5) Can our method achieve performance beyond the ceiling?

4.1 Experimental Setup

Dataset and Partition We conduct experiments on three datasets: **OpenImage** (Kuznetsova et al. 2020), **DomainNet** (Peng et al. 2019) and **NICO++** (Zhang et al. 2022b). All datasets consist of large-scale real-world images with the resolution of 224x224 pixels. DomainNet comprises six domains: *clipart*, *infograph*, *painting*, *quickdraw*, *real*, and *sketch*. Due to the distinct characteristics of *quickdraw* and the time cost of generation, we conduct experiments on the remaining five domains and each domain has the first 90 categories. For OpenImage, we follow a similar partition as (Yang et al. 2023), dividing the dataset into 20 superclasses based on the hierarchy of categories provided by OpenImage. Each superclass consists of 6 different fine-grained subclasses as 6 domains. Each domain has a fine-grained subclass of each superclass. The detailed partition can be found in supplementary materials. NICO++ involves 60 categories, with each category having six common domains shared across categories and six unique domains specific to each category. These two

Unique NICO++							
	client0	client1	client2	client3	client4	client5	Avg
Ceiling	74.02	78.90	79.68	74.47	77.34	77.47	76.98
SD_Gen	67.38	71.88	67.70	64.19	63.41	63.28	66.31
FedAvg	34.96	58.98	38.41	63.41	45.44	59.76	50.16
FedDF	51.85	52.34	55.85	52.47	54.42	59.24	54.36
FedCADO_FT	73.30	71.48	68.97	69.71	72.91	65.49	70.31
FedCADO_SD	67.77	76.04	73.95	70.44	76.56	68.35	72.19
Common NICO++							
	client0	client1	client2	client3	client4	client5	Avg
Ceiling	50.24	54.36	63.35	64.82	61.99	65.09	59.98
SD_Gen	38.64	45.55	53.08	54.72	50.19	59.91	50.35
FedAvg	18.23	27.79	36.32	52.42	37.96	39.24	35.33
FedDF	31.40	32.22	43.73	45.19	36.01	43.08	38.61
FedCADO_FT	58.98	46.53	60.93	57.45	53.92	54.32	55.36
FedCADO_SD	39.27	52.63	57.52	59.84	65.11	64.98	56.56

Table 2: Performance of different methods on Unique NICO++ and Common NICO++ under label distribution skew.

DomainNet							
\mathcal{L}_{BN}	\mathcal{L}_{CLS}	editing s_T	clipart	infograph	painting	real	sketch
✓			35.25	11.74	37.65	64.78	23.96
	✓		42.13	17.42	39.25	65.13	30.42
✓	✓		48.77	19.36	42.78	67.83	38.72
✓	✓	✓	51.86	22.11	48.63	68.96	41.73

Table 3: Results of the ablation experiments.

scenarios are respectively referred to as the **Unique NICO++** and **Common NICO++** datasets.

We validate our method in both feature distribution skew and label distribution skew scenarios. To simulate Feature Distribution Skew, we maintain the same label space while dividing the feature space into different clients. Each domain of these datasets serves as a client. To simulate label distribution skew, we partition the 60 categories of Common NICO++ into six clients, with each client containing different 10 categories. The same method is applied to partitioning Unique NICO++ into six clients. For fairness in comparisons between generated images and client images, we set the number of images per category to 30 for all clients. This setup mirrors real-world scenarios such as mobile photo classification and autonomous driving where clients often lack sufficient labeled data, as discussed in the introduction.

Regarding the text prompts used for guidance during the generation process, in the FL setup, the label space is publicly available to both the server and any client. The server naturally possesses the textual information of each label. However, it's challenging for the clients to provide textual descriptions of their personalized distributions. Therefore, to enhance the practicality of our method, we refrain from using any descriptions of client-specific distributions and solely employ the textual information of the class labels.

Baselines We primarily compare **FedCADO_FT** (Fine-Tuning), **FedCADO_MD** (Multi-teacher Distillation) and **FedCADO_SD** (Specific-teacher Distillation), against four baseline methods: 1) **FedAvg** (McMahan et al. 2017). The communication round of FedAvg is 20 in our experiments. 2) **FedDF** (Lin et al. 2020). Due to that FedDF needs a public dataset for distillation, we utilize the entire ImageNet (Deng et al. 2009) in our experiments. 3) **SD_Gen**. This baseline refers to the method where the generation is not guided by

Unique NICO++							
	client0	client1	client2	client3	client4	client5	Avg
Ceiling	83.07	84.89	84.11	80.85	84.76	84.47	83.69
SD_Gen	76.56	76.43	77.08	70.05	75.78	71.77	74.61
FedDF	71.09	70.57	67.96	66.67	62.11	52.34	65.12
FedCADO_FT	81.77	76.56	79.68	75.03	76.82	77.24	77.85
FedCADO_MD	81.64	81.91	82.55	81.89	82.94	75.48	81.07
FedCADO_SD	81.38	79.68	82.03	76.63	79.42	74.31	78.91
Common NICO++							
	client0	client1	client2	client3	client4	client5	Avg
Ceiling	70.25	60.98	70.28	68.45	68.01	59.97	66.32
SD_Gen	66.68	50.52	67.42	59.73	62.50	52.42	59.88
FedDF	49.97	43.37	60.05	55.12	53.75	51.17	52.24
FedCADO_FT	65.06	57.33	69.47	63.64	66.01	57.34	63.14
FedCADO_MD	68.19	57.55	71.46	66.28	67.18	58.82	64.91
FedCADO_SD	64.62	55.51	66.66	61.89	62.40	55.26	61.06

Table 4: Performance of different methods on Unique NICO++ and Common NICO++ with heterogeneous client models under feature distribution skew.

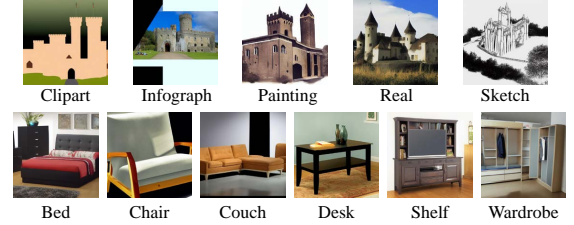


Figure 2: Generated samples and their corresponding domain labels on DomainNet and OpenImage.

any classifiers but only by the text prompts of class labels. 4) **Ceiling**. As mentioned in Section 1, this inaccessible baseline involves uploading all the client data to the server for centralized training of the aggregated model, completely disregarding privacy preservation.

It is important to note that, we also compare FedCADO with DENSE (Zhang et al. 2022a) and FedCVAE (Heinbaugh, Luz-Ricca, and Shao 2022). However, due to the reasons highlighted in Section 1, they exhibit poor adaptability to the datasets we used. The generator training struggles to converge. Furthermore, these methods primarily demonstrate results on smaller datasets like MNIST and CIFAR-10 in their paper without referential value for our experiments. Therefore, these methods are not utilized here.

4.2 Main Results

Experiments on Feature Distribution Skew Firstly, we conduct experiments to assess our method under feature distribution skew. From the results in Table 1, we can observe the following trends: 1) FedCADO consistently demonstrates superior performance across all datasets. 2) In multiple data domains, such as *real* domain of DomainNet and most domains of OpenImage, our approach exhibits performance surpassing the ceiling, which confirms our proposition in Section 1 that our method holds the potential to outperform the traditional FL framework's ceiling performance. The reason for the performance on these distributions is attributed to that the pre-trained DM we used was mainly pre-trained on realistic images, resulting in better generation performance for images that comply with these domains. 3) The direct



Figure 3: Comparison of generated samples along with their domain labels and original client images on Unique NICO++ and Common NICO++.

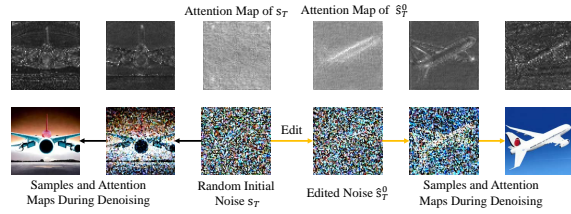


Figure 4: Comparison of the generation processes with and without editing for the same initial noise. The given category and distribution are *airplane* and *clipart*.

generation method shows promising performance on certain domains, like the *Real* domain, but underperforms on other domains. This is mainly attributed to the DM’s inclination to generate data that comply with the most common distribution in pre-training when solely the class label is provided, which emphasizes the necessity of additional guidance.

To validate the generating ability of our method, we present visualization results in Figure 2 and Figure 3, illustrating that FedCADO successfully generates images that possess accurate semantic information, comply with the specified client distribution, and exhibit competitive quality comparable to the original client datasets, which further confirms the excellent performance of our method in Table 1.

Experiments on Label Distribution Skew To validate the performance of FedCADO under label distribution skew, we conduct experiments on Unique and Common NICO++. The specific results are presented in Table 2. From the table, it is evident that FedCADO again shows the best performance. It is noticeable in Common NICO++’s client 0 and client 4, where it displays a performance improvement of over 3 percent beyond the ceiling. These results underscore the impressive performance of FedCADO under this scenario.

Experiments on Heterogeneous Models Table 4 shows that FedCADO can effectively perform heterogeneous model aggregation within a single communication round, showing performance close to the ceiling. These results demonstrate that FedCADO does not restrict the specific structures used by each client, further enhancing its practicality.

Ablation Experiments We also conduct ablation experiments to validate the effects of incorporating both BN loss and classification loss to guide image generation, as well as the addition of initial noise editing before denoising. From these results presented in Table 3, we can observe that:

- FedCADO with all the proposed factors achieves the best performance. The introduction of each factor progressively enhances the performance of our method.
- The performance is notably bad when only BN loss is used, which is worse than SD_Gen. This is primarily due to that BN loss lacks explicit category information, leading to unstable results with erroneous semantics.
- Relying solely on classification loss for guidance also fails to achieve ideal results. The primary role of the classification loss is to ensure semantic information preservation. As mentioned in Section 3.2, this confirms the difficulty of traditional classifier-guidance in the FL scenario, where both accurate categories and compliance with specific client distributions are required.
- Incorporating the initial noise editing leads to performance improvements. Additionally, the visual experiments in Figure 4 illustrate that the edited initial noise effectively guides the DM’s attention, which means the initial noise editing successfully embeds the specified semantic and distributional information into the initial noise, greatly enhancing the stability and quality of generation.

These observations collectively support the motivations mentioned in Section 1, proving the effectiveness of the various components of FedCADO in handling different challenges within the FL scenario.

4.3 Privacy Protection.

This paper follows the standard FL paradigm, sharing only client model updates without disclosing clients’ original data. Furthermore, we perform a single communication round. As discussed in (Zhang et al. 2022a), transmitting the parameters once alone can mitigate privacy leakage. Hence, our approach exhibits a reduced possibility of privacy leakage no matter in comparison to other OSFL methods requiring additional data transmission or generator training, or the other FL methods with the requirement of multi-round iteration. To further avoid the risk of privacy leaks, the privacy-preserving algorithms designed for protecting model parameters in other FL contexts (Abadi et al. 2016) are orthogonal to the focus of this paper. In practical application scenarios, there is potential to combine these privacy techniques with our research.

5 Conclusion

In this paper, we leverage the classifier-guided DMs to establish a powerful OSFL framework. Compared to existing methods, we eliminate the need for auxiliary datasets and generator training, making it effortlessly applicable in real-world complex scenarios. Comprehensive experiments on three large-scale datasets demonstrate that the proposed FedCADO surpasses all baseline methods and achieves performance close to the ceiling in certain experiments. In summary, FedCADO unveils unprecedented practicality for OSFL.

References

- Abadi, M.; Chu, A.; Goodfellow, I.; McMahan, H. B.; Mironov, I.; Talwar, K.; and Zhang, L. 2016. Deep learning with differential privacy. In *Proceedings of the 2016 ACM SIGSAC conference on computer and communications security*, 308–318.
- Deng, J.; Dong, W.; Socher, R.; Li, L.-J.; Li, K.; and Fei-Fei, L. 2009. Imagenet: A large-scale hierarchical image database. In *2009 IEEE conference on computer vision and pattern recognition*, 248–255. Ieee.
- Dhariwal, P.; and Nichol, A. 2021. Diffusion models beat gans on image synthesis. *Advances in neural information processing systems*, 34: 8780–8794.
- Fantauzzo, L.; Fanì, E.; Caldarola, D.; Tavera, A.; Cermelli, F.; Ciccone, M.; and Caputo, B. 2022. Feddrive: Generalizing federated learning to semantic segmentation in autonomous driving. In *2022 IEEE/RSJ International Conference on Intelligent Robots and Systems (IROS)*, 11504–11511. IEEE.
- Feng, W.; He, X.; Fu, T.-J.; Jampani, V.; Akula, A.; Narayana, P.; Basu, S.; Wang, X. E.; and Wang, W. Y. 2022. Training-free structured diffusion guidance for compositional text-to-image synthesis. *arXiv preprint arXiv:2212.05032*.
- Gu, S.; Chen, D.; Bao, J.; Wen, F.; Zhang, B.; Chen, D.; Yuan, L.; and Guo, B. 2022. Vector quantized diffusion model for text-to-image synthesis. In *Proceedings of the IEEE/CVF Conference on Computer Vision and Pattern Recognition*, 10696–10706.
- Guha, N.; Talwalkar, A.; and Smith, V. 2019. One-shot federated learning. *arXiv preprint arXiv:1902.11175*.
- Heinbaugh, C. E.; Luz-Ricca, E.; and Shao, H. 2022. Data-Free One-Shot Federated Learning Under Very High Statistical Heterogeneity. In *The Eleventh International Conference on Learning Representations*.
- Ho, J.; Jain, A.; and Abbeel, P. 2020. Denoising diffusion probabilistic models. *Advances in Neural Information Processing Systems*, 33: 6840–6851.
- Jothiraj, F. V. S.; and Mashhadi, A. 2023. Phoenix: A Federated Generative Diffusion Model. *arXiv preprint arXiv:2306.04098*.
- Kim, G.; Kwon, T.; and Ye, J. C. 2022. Diffusionclip: Text-guided diffusion models for robust image manipulation. In *Proceedings of the IEEE/CVF Conference on Computer Vision and Pattern Recognition*, 2426–2435.
- Kingma, D.; Salimans, T.; Poole, B.; and Ho, J. 2021. Variational Diffusion Models. In Ranzato, M.; Beygelzimer, A.; Dauphin, Y.; Liang, P.; and Vaughan, J. W., eds., *Advances in Neural Information Processing Systems*, volume 34, 21696–21707. Curran Associates, Inc.
- Kuznetsova, A.; Rom, H.; Alldrin, N.; Uijlings, J.; Krasin, I.; Pont-Tuset, J.; Kamali, S.; Popov, S.; Mallocci, M.; Kolesnikov, A.; et al. 2020. The open images dataset v4: Unified image classification, object detection, and visual relationship detection at scale. *International Journal of Computer Vision*, 128(7): 1956–1981.
- Li, J.; Li, D.; Savarese, S.; and Hoi, S. 2023. Blip-2: Bootstrapping language-image pre-training with frozen image encoders and large language models. *arXiv preprint arXiv:2301.12597*.
- Li, Q.; He, B.; and Song, D. 2020. Practical one-shot federated learning for cross-silo setting. *arXiv preprint arXiv:2010.01017*.
- Lin, T.; Kong, L.; Stich, S. U.; and Jaggi, M. 2020. Ensemble distillation for robust model fusion in federated learning. *Advances in Neural Information Processing Systems*, 33: 2351–2363.
- Liu, L.; Ren, Y.; Lin, Z.; and Zhao, Z. 2022. Pseudo numerical methods for diffusion models on manifolds. *arXiv preprint arXiv:2202.09778*.
- Mao, J.; Wang, X.; and Aizawa, K. 2023. Guided Image Synthesis via Initial Image Editing in Diffusion Model. *arXiv preprint arXiv:2305.03382*.
- McMahan, B.; Moore, E.; Ramage, D.; Hampson, S.; and y Arcas, B. A. 2017. Communication-efficient learning of deep networks from decentralized data. In *Artificial Intelligence and Statistics*, 1273–1282. PMLR.
- Nguyen, A.; Do, T.; Tran, M.; Nguyen, B. X.; Duong, C.; Phan, T.; Tjiputra, E.; and Tran, Q. D. 2022. Deep federated learning for autonomous driving. In *2022 IEEE Intelligent Vehicles Symposium (IV)*, 1824–1830. IEEE.
- Nichol, A.; Dhariwal, P.; Ramesh, A.; Shyam, P.; Mishkin, P.; McGrew, B.; Sutskever, I.; and Chen, M. 2021. Glide: Towards photorealistic image generation and editing with text-guided diffusion models. *arXiv preprint arXiv:2112.10741*.
- Peng, X.; Bai, Q.; Xia, X.; Huang, Z.; Saenko, K.; and Wang, B. 2019. Moment matching for multi-source domain adaptation. In *Proceedings of the IEEE/CVF international conference on computer vision*, 1406–1415.
- Preechakul, K.; Chatthee, N.; Wizadwongsa, S.; and Suwajanakorn, S. 2022. Diffusion autoencoders: Toward a meaningful and decodable representation. In *Proceedings of the IEEE/CVF Conference on Computer Vision and Pattern Recognition*, 10619–10629.
- Rombach, R.; Blattmann, A.; Lorenz, D.; Esser, P.; and Ommer, B. 2022. High-resolution image synthesis with latent diffusion models. In *Proceedings of the IEEE/CVF Conference on Computer Vision and Pattern Recognition*, 10684–10695.
- Saharia, C.; Chan, W.; Chang, H.; Lee, C.; Ho, J.; Salimans, T.; Fleet, D.; and Norouzi, M. 2022a. Palette: Image-to-image diffusion models. In *ACM SIGGRAPH 2022 Conference Proceedings*, 1–10.
- Saharia, C.; Chan, W.; Saxena, S.; Li, L.; Whang, J.; Denton, E. L.; Ghasemipour, K.; Gontijo Lopes, R.; Karagol Ayan, B.; Salimans, T.; et al. 2022b. Photorealistic text-to-image diffusion models with deep language understanding. *Advances in Neural Information Processing Systems*, 35: 36479–36494.
- Sohl-Dickstein, J.; Weiss, E.; Maheswaranathan, N.; and Ganguli, S. 2015. Deep unsupervised learning using nonequilibrium thermodynamics. In *International Conference on Machine Learning*, 2256–2265. PMLR.

Song, J.; Meng, C.; and Ermon, S. 2020. Denoising diffusion implicit models. *arXiv preprint arXiv:2010.02502*.

Song, Y.; Sohl-Dickstein, J.; Kingma, D. P.; Kumar, A.; Ermon, S.; and Poole, B. 2020. Score-based generative modeling through stochastic differential equations. *arXiv preprint arXiv:2011.13456*.

Su, S.; Li, B.; and Xue, X. 2023. One-shot Federated Learning without server-side training. *Neural Networks*, 164: 203–215.

Su, X.; Song, J.; Meng, C.; and Ermon, S. 2022. Dual diffusion implicit bridges for image-to-image translation. In *The Eleventh International Conference on Learning Representations*.

Wang, T.; Zhang, T.; Zhang, B.; Ouyang, H.; Chen, D.; Chen, Q.; and Wen, F. 2022. Pretraining is all you need for image-to-image translation. *arXiv preprint arXiv:2205.12952*.

Wang, T.-C.; Liu, M.-Y.; Zhu, J.-Y.; Tao, A.; Kautz, J.; and Catanzaro, B. 2018. High-resolution image synthesis and semantic manipulation with conditional gans. In *Proceedings of the IEEE conference on computer vision and pattern recognition*, 8798–8807.

Xie, J.; Li, Y.; Huang, Y.; Liu, H.; Zhang, W.; Zheng, Y.; and Shou, M. Z. 2023. BoxDiff: Text-to-Image Synthesis with Training-Free Box-Constrained Diffusion. *arXiv preprint arXiv:2307.10816*.

Yang, M.; Su, S.; Li, B.; and Xue, X. 2023. Exploring One-shot Semi-supervised Federated Learning with A Pre-trained Diffusion Model. *arXiv preprint arXiv:2305.04063*.

Zhang, J.; Chen, C.; Li, B.; Lyu, L.; Wu, S.; Ding, S.; Shen, C.; and Wu, C. 2022a. Dense: Data-free one-shot federated learning. *Advances in Neural Information Processing Systems*, 35: 21414–21428.

Zhang, J.; Qi, X.; and Zhao, B. 2023. Federated Generative Learning with Foundation Models. *arXiv preprint arXiv:2306.16064*.

Zhang, L.; and Agrawala, M. 2023. Adding conditional control to text-to-image diffusion models. *arXiv preprint arXiv:2302.05543*.

Zhang, X.; Zhou, L.; Xu, R.; Cui, P.; Shen, Z.; and Liu, H. 2022b. Nico++: Towards better benchmarking for domain generalization. *arXiv preprint arXiv:2204.08040*.

Zhou, Y.; Pu, G.; Ma, X.; Li, X.; and Wu, D. 2020. Distilled one-shot federated learning. *arXiv preprint arXiv:2009.07999*.

In the supplementary materials, we first provide the pseudocode and some details of our method. Subsequently, we delve into additional descriptions of the dataset and implementation details in our experiments. Lastly, we further illustrate the performance and credibility of FedDISC by presenting additional visualization experiments.

A Method Details

Our method focuses on the one-shot federated learning scenario, as depicted in Figure 5. In this setting, all clients initially train their own classifiers and upload them to the server. Based on these classifiers, the server obtains an aggregated model that adapts to all client distributions. The pseudocode for our method, as well as the method overview in Figure 1 of the main text, starts from the received classifiers.

A.1 Pseudocode

The pseudocode for FedCADO is presented in Algorithm 1. Please refer to the pseudocode provided here for the comprehensive algorithmic flow. The loop involving m represents the process of editing initial noise, while the loop involving T signifies the denoising diffusion process.

A.2 Model Structure

Specifically, the model we employ in FedCADO consists of a pre-trained Stable Diffusion, which is composed of a VAE and an Unet, along with a classification model with arbitrary structure. The overall model architecture is depicted in Figure 6. All model parameters remain fixed during the generation of synthetic datasets. Gradients are backpropagated from the classifiers to the input noise, guiding the process of initial noise editing and diffusion denoising.

B Details of Experiments

In this section, we provide further experimental details, including the specific selection of superclasses and fine-grained subclasses in OpenImage, the exact quantities of images in the training and testing sets of each dataset, as well as implementation details.

B.1 Selection of Superclasses

For OpenImage, we follow a similar partition as (Yang et al. 2023), dividing the dataset into 20 superclasses based on the hierarchy of categories provided by OpenImage. Each superclass consists of 6 different fine-grained subclasses as 6 domains. Each domain has a fine-grained subclass of each superclass. The detailed partition can be found in Table 5.

B.2 Implementation Details

Regarding the used model structure, by default, we use ResNet18 as the local client classifier’s structure and the aggregated model’s structure. In the experiment with heterogeneous models, the structures of the local classifiers are MobileNetV3, ResNet18, ResNet34, MobileNetV2, VGG16, and ShuffleNet, and the structure of the aggregated model is ResNet50. For the diffusion model used in image generation, we utilize the Stable Diffusion v1.5 (Rombach et al. 2022), available on *HuggingFace*. All experiments are completed

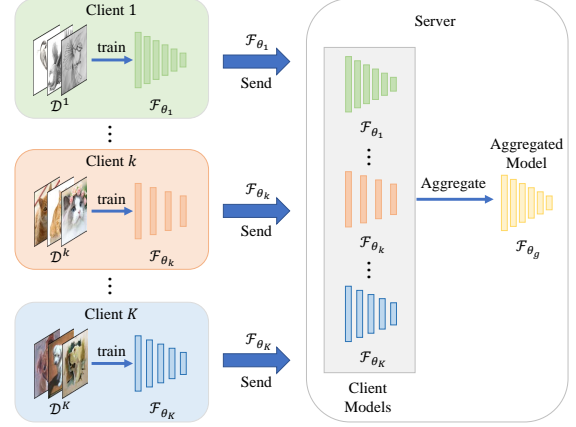


Figure 5: The overview of one-shot federated learning scenario. In realistic applications, it’s common to encounter three complex scenarios among various clients: feature distribution skew, label distribution skew, and heterogeneity in client model structures. All these intricate scenarios have been meticulously addressed and covered in our experiments.

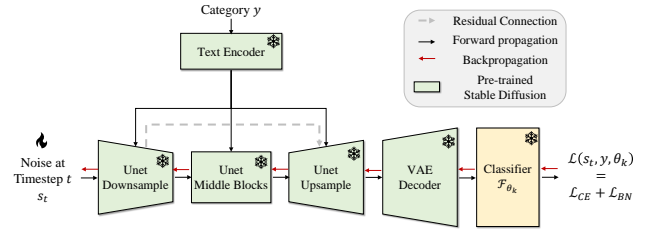


Figure 6: The overall model structure used in FedCADO consists of the pre-trained Stable Diffusion ϵ_θ and local classifiers $\{\mathcal{F}_{\theta_k}\}_{k=1}^K$.

with four NVIDIA GeForce RTX 3090 GPUs. Regarding specific hyperparameters, the number of steps for editing the initial noise (M) is set to 10. The weight of BN Loss λ is 0.1. The learning rate of initial noise editing η is 0.1. About the image quantity of synthetic dataset $\hat{\mathbf{X}}$, we generate 30 images for each class in each distribution. The local classifiers and the final aggregated model are trained for 20 epochs with a learning rate of 0.01. The guidance scale of Stable Diffusion is 3.

B.3 Image Quantities

As mentioned in the main text, our experiments involve a direct comparison between generated datasets and original client datasets. Due to the cost factor associated with generating images, we created only 30 images per category for each class on every client. To ensure fairness in image quantity for comparison, we also randomly selected 30 images per category from the original training set of each client. While the count of 30 images per category may appear limited, it is sufficient for training local client classifiers and guiding

Algorithm 1: FedCADO: a Classifier-Assisted Diffusion for One-shot Federated learning method

Input: The local client classifiers $\{\mathcal{F}_{\theta_k}\}_{k=1}^K$. A pre-trained diffusion model ϵ_θ .

Output: An aggregated model \mathcal{F}_{θ_g} adapted to the data distributions of all client datasets $\mathcal{D}^k = \{(\mathbf{x}_i, y_i)\}_{i=1}^{N_k}, y_i \in \{1, \dots, C\}$.

```

1: create empty synthetic dataset  $\hat{\mathbf{X}} = \{\}$ 
2: for domain label  $k = 1, \dots, K$  do
3:   for number of synthetic images  $i = 1, \dots, N$  do
4:     randomly select a category  $y$  supported by the client classifier  $\mathcal{F}_{\theta_k}$ .
5:     randomly sample the initial noise  $\hat{\mathbf{s}}_T^M$  from  $\mathcal{N}(0, \mathcal{I})$ .
6:     for  $m = M, \dots, 0$  do
7:       use  $\epsilon_\theta$  to compute  $\epsilon_\theta(\hat{\mathbf{s}}_T^m, T|y)$ 
8:        $\hat{\mathbf{s}}_{0,T}^m \leftarrow \frac{\hat{\mathbf{s}}_T^m - \sqrt{1-\alpha_T}\epsilon_\theta(\hat{\mathbf{s}}_T^m, T|y)}{\sqrt{\alpha_T}}$ 
9:        $\mathcal{L}(\hat{\mathbf{s}}_T^m, y, \theta_k) \leftarrow \mathcal{L}_{CE}(\mathcal{F}_{\theta_k}(\hat{\mathbf{s}}_{0,T}^m, y) + \lambda \mathcal{L}_{BN}(\hat{\mathbf{s}}_{0,T}^m, \theta_k)$ 
10:       $\hat{\mathbf{s}}_T^{m-1} \leftarrow \hat{\mathbf{s}}_T^m - \eta \nabla_{\hat{\mathbf{s}}_T^m} \mathcal{L}(\hat{\mathbf{s}}_T^m, y, \theta_k)$ .
11:    end for
12:     $\mathbf{s}_T \leftarrow \hat{\mathbf{s}}_T^0$ 
13:    for  $t = T, \dots, 0$  do
14:      use  $\epsilon_\theta$  to compute  $\epsilon_\theta(\mathbf{s}_t, t|y)$ 
15:       $\hat{\mathbf{s}}_{0,t} \leftarrow \frac{\mathbf{s}_t - \sqrt{1-\alpha_t}\epsilon_\theta(\mathbf{s}_t, t|y)}{\sqrt{\alpha_t}}$ 
16:      compute  $\mathcal{L}(\mathbf{s}_t, y, \theta_k)$  by Eq. (4).
17:      compute  $\hat{\epsilon}(\mathbf{s}_t, t|y)$  by Eq. (5).
18:      compute  $\mathbf{s}_{t-1}$  by Eq. (2).
19:    end for
20:     $(\hat{\mathbf{x}}_i^k, y_i^k) \leftarrow (\mathbf{s}_0, y)$ 
21:    add  $(\hat{\mathbf{x}}_i^k, y_i^k)$  to synthetic dataset  $\hat{\mathbf{X}}$ 
22:  end for
23: end for
24: use  $\hat{\mathbf{X}} = \{(\hat{\mathbf{x}}_i^k, y_i^k)\}_{i=1}^N, k = 1, \dots, K$  to train an aggregated model  $\mathcal{F}_{\theta_g}$  by fine-tuning, multi-teacher distillation or
    specific-teacher distillation based on Eq. (6) as described in Section 3.4.
25: return the aggregated model  $\mathcal{F}_{\theta_g}$ 

```

the generation of synthetic datasets on the server. This setup is more aligned with real-world scenarios, as disparities in image quantity among clients are common, reflecting situations where certain clients possess only a limited number of images. Yet, we must still strive to extract the desired information from these clients.

All experimental results underwent cross-fold validation, with the reported results being averages across multiple tests. For the DomainNet dataset, in each experiment, we used all images except the chosen 30 training images as the testing set, to perform cross-validation. Regarding OpenImage and NICO++, since these datasets already have predefined test and training sets, we incorporated images from the training set in each experiment for client inclusion, and we consistently used all test set images for performance validation. Specific image quantities can be referenced in Table 6.

C Additional Experiments

In this section, we primarily provide additional visualization experiments showcasing the generated synthetic datasets. These experiments aim to illustrate our claim that FedDISC can indeed generate images that comply with personalized client distributions while maintaining accurate semantic content. Furthermore, we illustrate that the synthetic dataset pos-

sesses diversity and quality on par with, or even overpasses, the original client dataset. We mainly conduct visualization experiments in two aspects: the image quality and the image diversity.

C.1 Image Quality

In Figures 3 and 4, we present more visual experiments conducted on the DomainNet dataset. These visualizations primarily focus on the feature distribution skew scenario, with five domains in DomainNet representing five clients, excluding the *quickdraw* domain.

The reason for not considering the *quickdraw* domain in our experiments is primarily due to the uniqueness of *quickdraw*. Stable diffusion currently faces challenges in generating images consistently complying with *quickdraw* domain, and the lack of clear semantics in these images can exacerbate the instability of the generation process, thus affecting the overall server aggregation process.

From the results, we can observe that FedCADO can generate synthetic datasets that comply with the personalized client distribution and are semantically accurate for most domains. The quality of the synthetic datasets approaches that of the original client dataset. The only domain where the generation is not as ideal is *infograph*. The main reason for this is the distinctiveness of the *infograph* domain, which mainly relies

Table 5: The selections of categories on the OpenImage dataset.

Super-category	Baked goods	Bird	Building	Carnivore	Clothing	Drink	Fruit	Furniture	Home appliance	Human body
Client0	Pretzel	Woodpecker	Convenience store	Bear	Shorts	Beer	Apple	Chair	Washing machine	Human eye
Client1	Bagel	Parrot	House	Leopard	Dress	Cocktail	Lemon	Desk	Toaster	Skull
Client2	Muffin	Magpie	Tower	Fox	Swimwear	Coffee	Banana	Couch	Oven	Human mouth
Client3	Cookie	Eagle	Office building	Tiger	Brassiere	Juice	Strawberry	Wardrobe	Blender	Human ear
Client4	Bread	Falcon	Castle	Lion	Tiara	Tea	Peach	Bed	Gas stove	Human nose
Client5	Croissant	Sparrow	Skyscraper	Otter	Shirt	Wine	Pineapple	Shelf	Mechanical fan	Human foot
Super-category	Kitchen utensil	Land vehicle	Musical instrument	Office supplies	Plant	Reptile	Sports equipment (Ball)	Toy	Vegetable	Weapon
Client0	Spatula	Ambulance	Drum	Pen	Maple	Dinosaur	Football	Doll	Potato	Knife
Client1	Spoon	Cart	Guitar	Poster	Willow	Lizard	Tennis ball	Balloon	Carrot	Axe
Client2	Fork	Bus	Harp	Calculator	Rose	Snake	Baseball bat	Dice	Broccoli	Sword
Client3	Knife	Van	Piano	Whiteboard	Lily	Tortoise	Golf ball	Flying disc	Cabbage	Handgun
Client4	Whisk	Truck	Violin	Box	Common sunflower	Crocodile	Rugby ball	Kite	Bell pepper	Shotgun
Client5	Cutting board	Car	Accordion	Envelope	Houseplant	Sea turtle	Volleyball (Ball)	Teddy bear	Pumpkin	Dagger

Table 6: The number of images in each dataset.

	Client0		Client1		Client2		Client3		Client4		Client5		Total	
	Train	Test	Train	Test	Train	Test	Train	Test	Train	Test	Train	Test	Train	Test
DomainNet 90 class	2646	8024	2449	7745	2543	14507	2700	41113	2686	41628	2575	11041	15599	124058
OpenImage	600	6856	600	8025	600	6761	600	6179	600	6397	600	7318	3600	41536
NICO++_C	1632	846	1733	1010	1669	1004	1697	929	1696	865	1751	1062	10178	5716
NICO++_U	1692	1819	1781	2498	1800	4066	1800	3338	1800	2213	1800	3841	10673	17775

on textual features. On one hand, client classification models trained on *infograph* focus more on image-related features rather than text, resulting in limited textual knowledge in the classifiers. On the other hand, stable diffusion currently exhibits weaknesses in generating textual information in images, leading to few recognizable textual elements in the generated images. These two factors lead to the synthesized dataset for the *infograph* domain closely resembling the original client dataset in the overall composition, but most of the generated images lack readable text, so the distribution between these two datasets is kind of different.

In Figure 5, we showcase visualizations of the synthetic datasets for OpenImage and Unique NICO++ experiments, which involve different fine-grained subclasses among clients. In Figure 6, we demonstrate visualizations for the Common NICO++ experiment, where clients have different backgrounds. These visualizations reveal that the synthetic datasets effectively capture various fine-grained subclasses and different client backgrounds, approaching the high quality of the original client datasets.

These visualizations sufficiently support the claim that FedCADO can generate large-scale, high-quality synthetic datasets that comply with personalized client distributions and maintain accurate semantics only with the received local classifiers, without direct access to any client data. Consequently, models trained on such synthetic datasets can achieve performance close to or surpass the performance ceiling of centralized training. These visual experiments robustly complement our various quantitative results.

C.2 Image Diversity

To demonstrate the advantages of the synthetic dataset in terms of image diversity, we have provided additional generated samples from the synthetic dataset in Figures 11 13 14. For comparison, we visualize the synthetic dataset generated by another baseline method that requires data generation: SD_GEN, as shown in Figure 12.

From the comparison between Figure 11 and Figure 12, it is evident that when no guidance is provided, even if the diffusion model can generate images with the target semantics, the images primarily comply with domain *real*, because the diffusion model is mainly pre-trained on the datasets comply with domain *real*. As a result, the images SD_GEN generates cannot comply with other client distributions just employing the diversity from the random sampling of initial noise. However, in the visual experiments of FedCADO, we can clearly observe that the images exhibit diverse styles that comply with various clients. This is absolutely challenging to achieve with the diffusion model alone without specific prompts, and there are hardly any similar images generated in the process, demonstrating strong diversity. Results in Figure 13 for DomainNet and Figure 14 for OpenImage also lead to similar conclusions.

In summary, we believe that FedCADO can generate large-scale synthetic datasets of realistic images without direct access to any client data, solely relying on the client-uploaded classifiers. These synthetic datasets are comparable, or even surpassing, the original client datasets in terms of image quality and diversity. Consequently, the aggregated models trained with FedCADO can achieve performance that even exceeds the ceiling of centralized training.

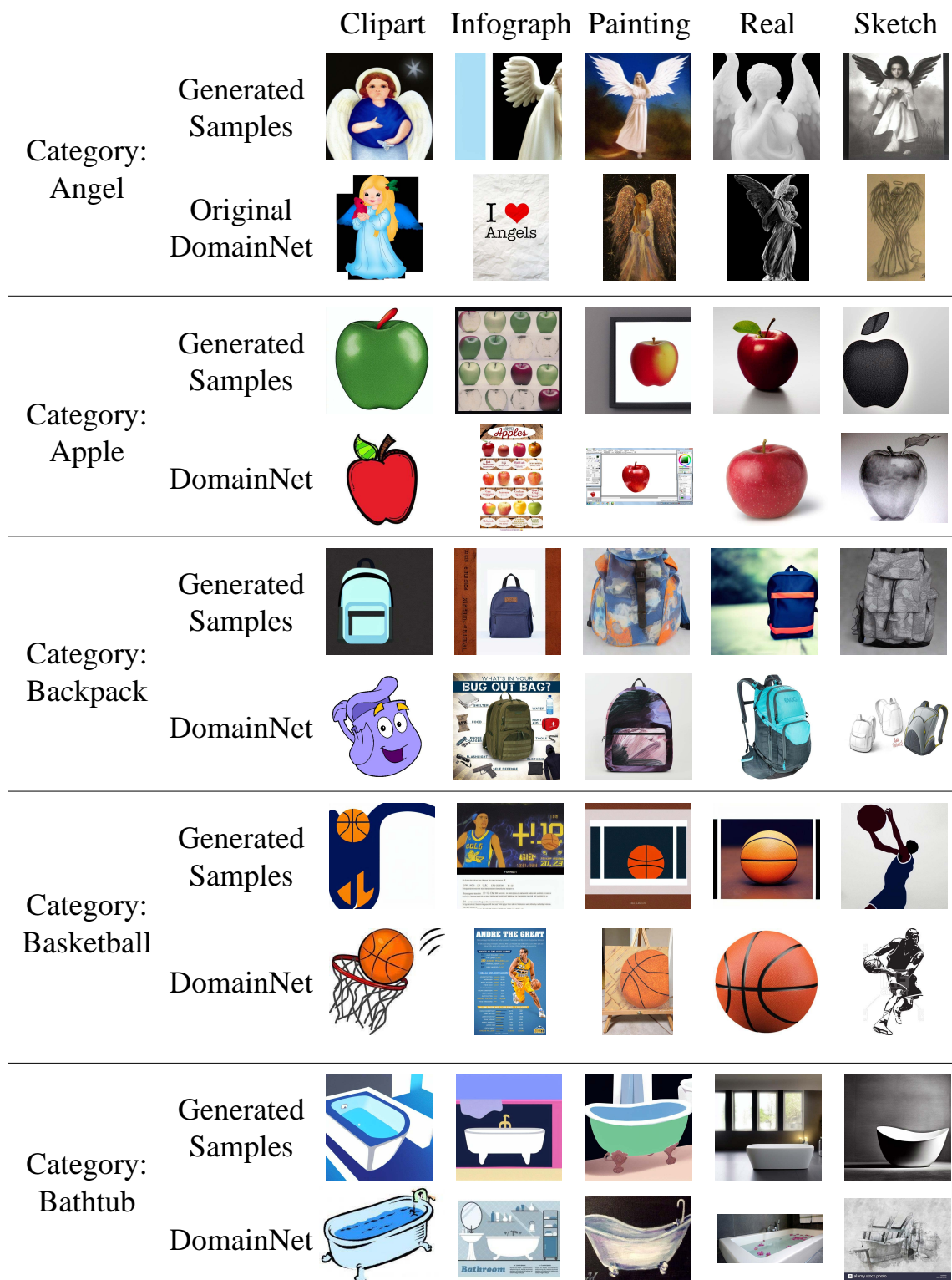


Figure 7: Comparison between the synthetic dataset and the original client dataset in the experiment on DomainNet.

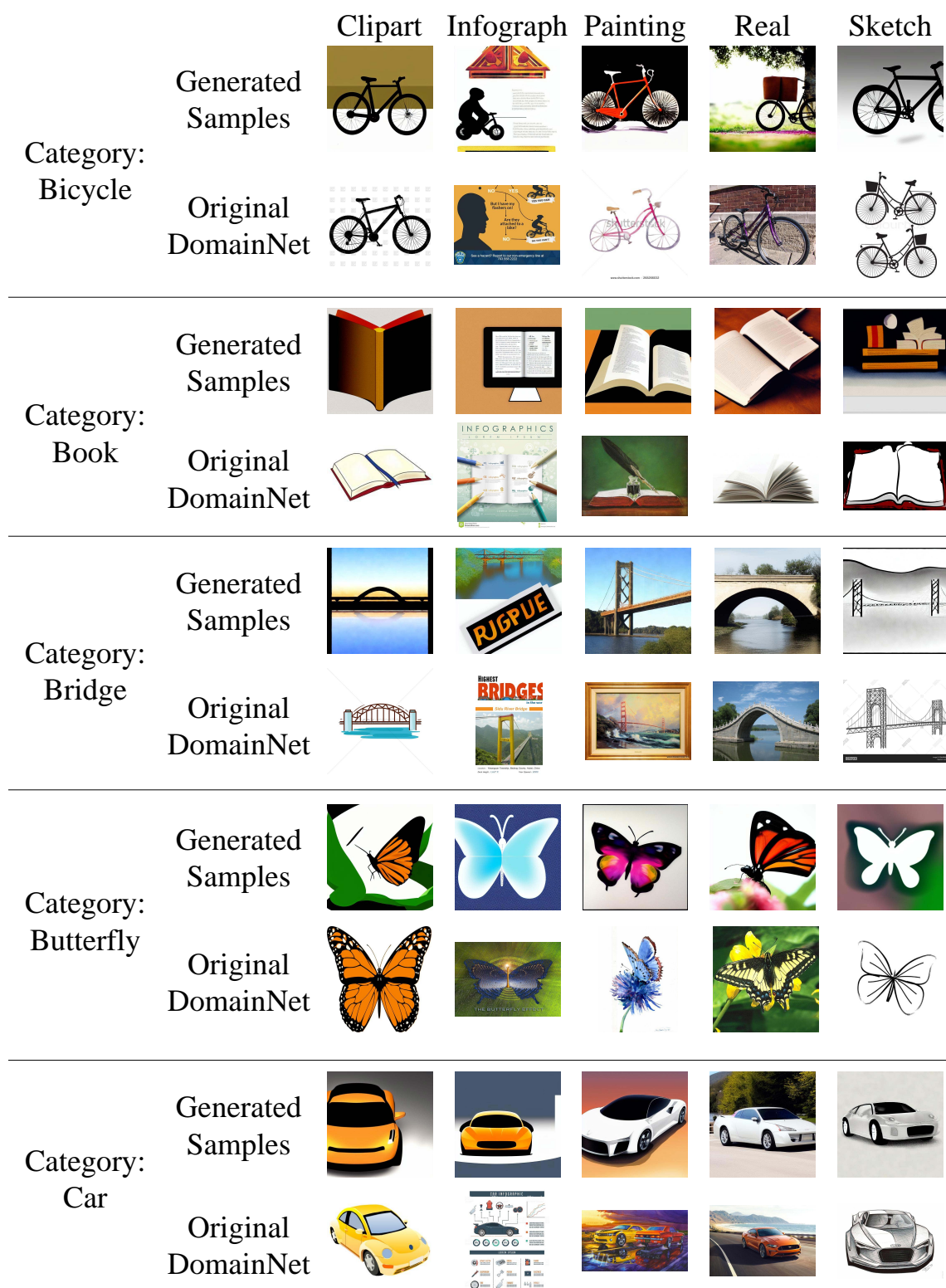


Figure 8: More comparison between the synthetic dataset and the original client dataset in the experiment on DomainNet.







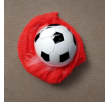

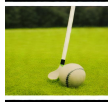



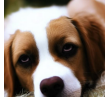
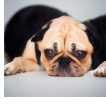
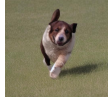
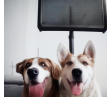
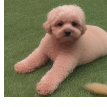







Superclass: Kitchen Utensil	Generated Samples	Spatula	Spoon	Fork	Knife	Whisk	Cutting Board
	Original OpenImage						
Superclass: Sports Equipment (Ball)	Generated Samples	Football	Tennis Ball	Baseball	Golf Ball	Rugby Ball	Volleyball
	Original OpenImage						
Superclass: Dog	Generated Samples	Lying	Pug Dog	Running	Skicking Out Tongue	Teddy Dog	Wearing Clothes
	Original Unique NICO++						
Superclass: Lifeboat	Generated Samples	Across Bridge	Enclosed	On Wave	White	With paddle	Yellow
	Original Unique NICO++						

Figure 9: Comparison between the synthetic dataset and the original client dataset in the experiments on OpenImage and Unique NICO++.

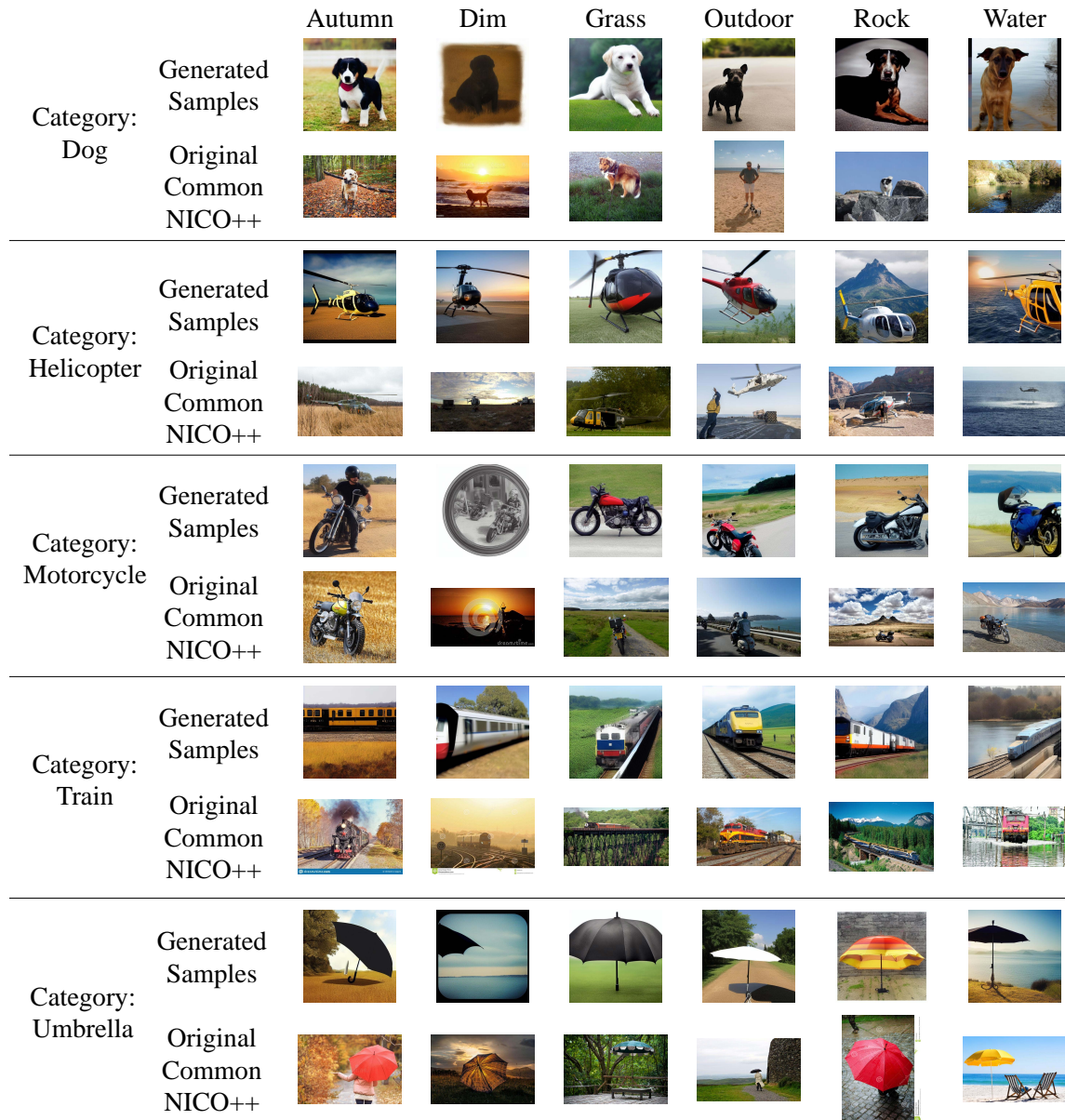


Figure 10: Comparison between the synthetic dataset and the original client dataset in the experiment on Common NICO++.

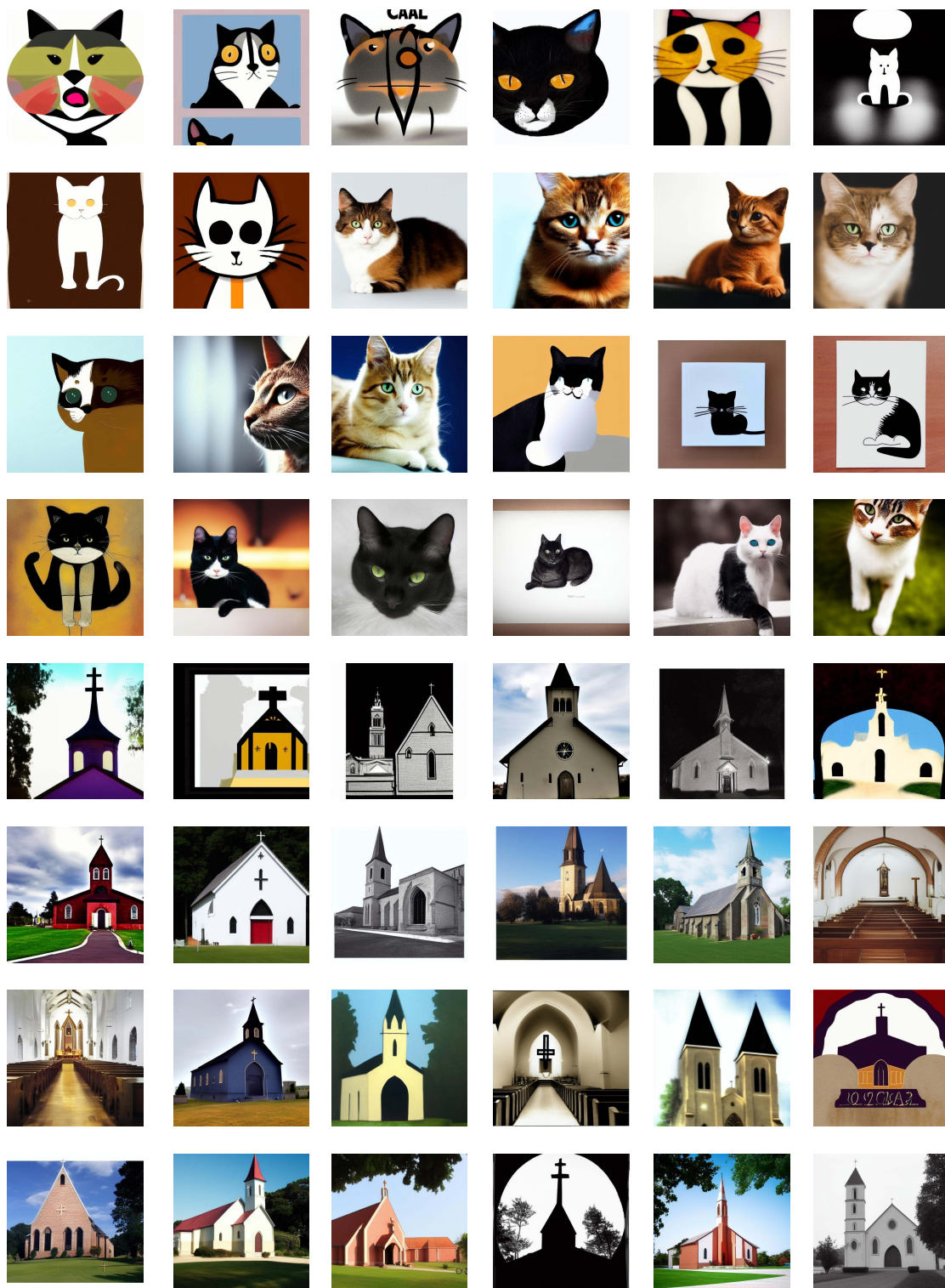


Figure 11: Generated samples of synthetic datasets corresponding to the experiment on DomainNet. The order of these images is random. It is evident that the generated images exhibit a high degree of diversity, spanning from style and composition to colors, backgrounds, and more. There are scarcely any two similar images among them.



Figure 12: Generated samples of SD_GEN's synthetic dataset on the experiments of DomainNet. Compared with the FedCADO's synthetic dataset, The distribution predominantly converges toward the most common domain, making it challenging to comply with client distributions, leading to a noticeable decrease in diversity.

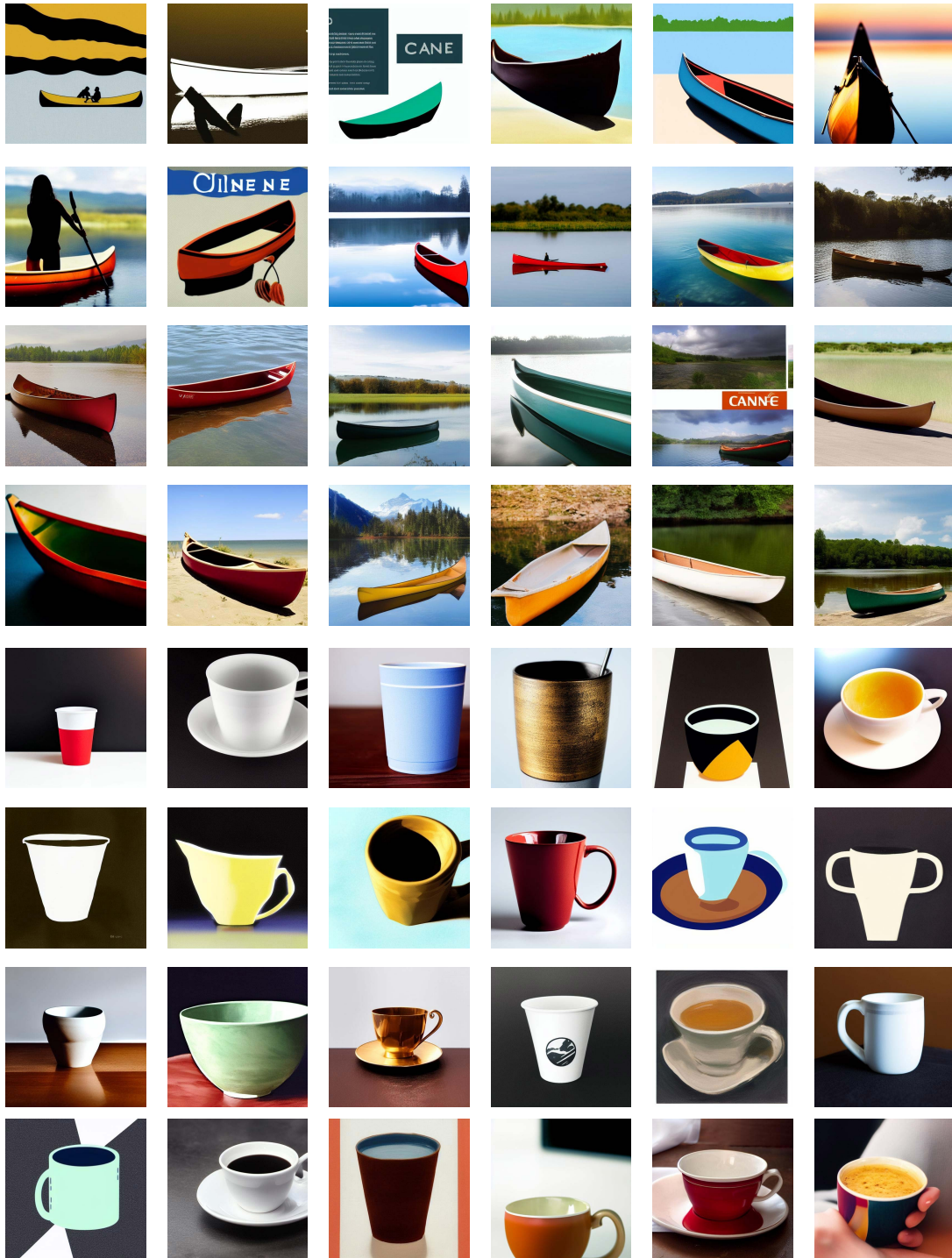


Figure 13: Generated samples of synthetic datasets corresponding to the experiment on DomainNet. The order of these images is random. It is evident that the generated images exhibit a high degree of diversity.

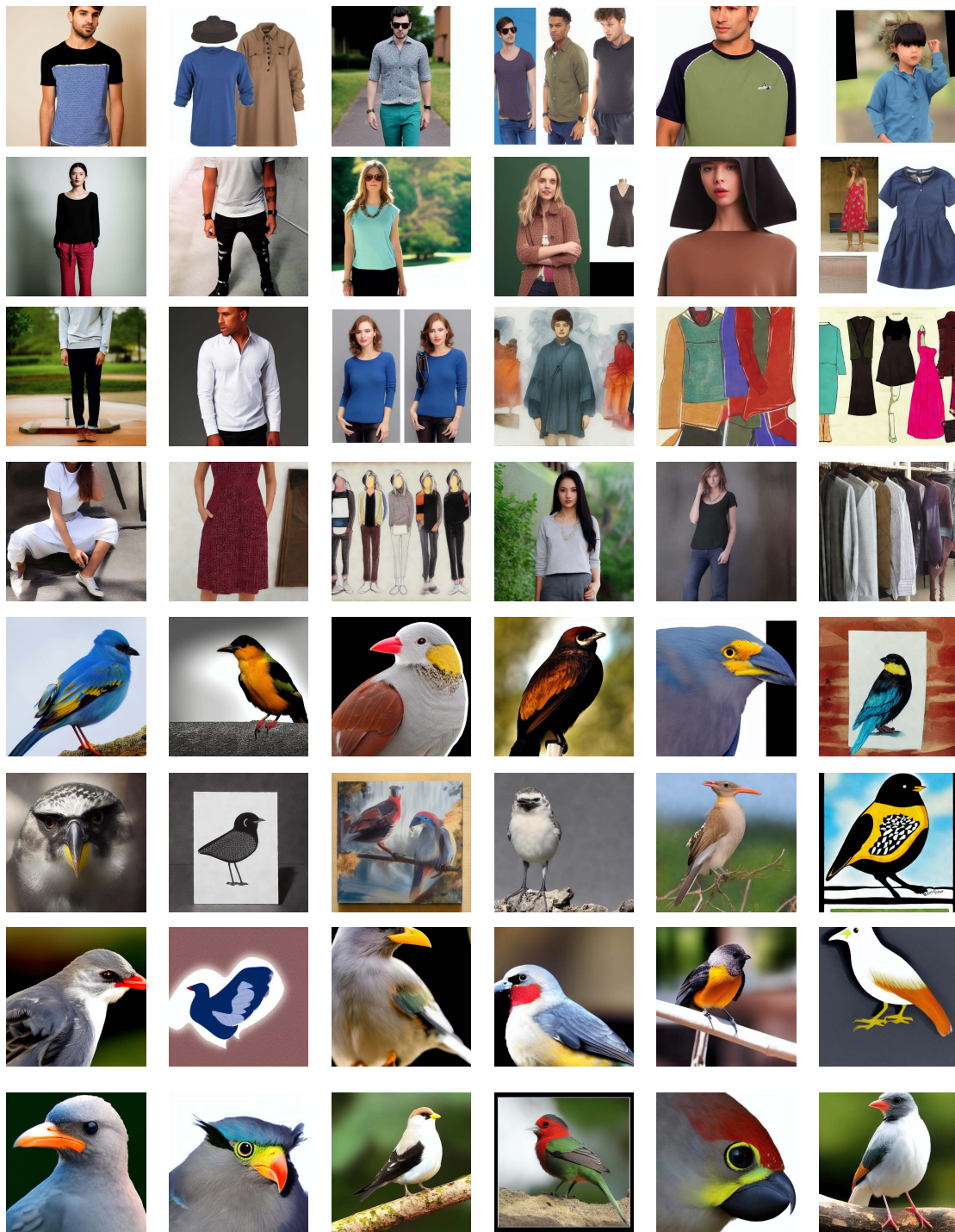


Figure 14: Generated samples of synthetic datasets corresponding to the experiment on OpenImage. The order of these images is random. It is evident that the generated images exhibit a high degree of diversity.